Renal Denervation Using Focused Infrared Fiber Lasers: A Potential Treatment for Hypertension

Vinay V. Alexander, PhD,[1*] Zhennan Shi, MSc,[1] Fariha Iftekher, BS,[1] Michael J. Welsh, PhD,[3] Hitinder S. Gurm, MD,[2] Gail Rising, LVT,[4] Amber Yanovich, LVT,[4] Kim Walacavage, BS,[4] and Mohammed N. Islam, PhD[1,2]

[1]*Electrical and Computer Engineering Department, University of Michigan, Ann Arbor, Michigan 48109*
[2]*Department of Internal Medicine, University of Michigan Medical School, Ann Arbor, Michigan 48109*
[3]*Department of Cell and Developmental Biology, University of Michigan, Ann Arbor, Michigan 48109*
[4]*Unit for Laboratory and Animal Medicine, University of Michigan Medical School, Ann Arbor, Michigan 48109*

Background and Objective: Renal denervation has recently become of great interest as a potential treatment for resistant hypertension. Denervation techniques using radio frequency (RF) or ultrasound energy sources have already been explored in literature. In this study, we investigate the use of lasers as a potential energy source for renal denervation. In vitro studies are performed in porcine/ovine renal arteries with focused laser beams at 980 nm, 1210 nm, and 1700 nm to study the ability to damage renal nerves without causing injury to non-target tissue structures like the endothelium. Then, a 980 nm laser catheter prototype is built and used to demonstrate *in vivo* renal denervation in ovine renal arteries.

Subjects and Methods: This study utilizes fiber coupled infrared lasers at 980 nm, 1210 nm, and 1700 nm. In vitro laser denervation studies at 980 nm are performed in both porcine and ovine renal arteries to study the ability of focused laser beams to damage renal nerves without injuring the endothelium. In vitro studies using lasers close to the lipid absorption lines at 1210 nm and 1700 nm are also performed in porcine renal arteries to study the possibility of selectively damaging the renal nerves by targeting the lipid myelin sheaths surrounding the nerves. Then, a laser catheter prototype is designed and built for *in vivo* renal denervation in ovine renal arteries using the 980 nm laser (powers ranging from 2 to 4 W, 5 seconds per exposure). Histochemical evaluations of the frozen sections are performed using methylthiazolyldiphenyl-tetrazolium bromide (MTT) assay.

Results: Histochemical analysis of *in vitro* laser treatments at 980 nm in porcine and ovine renal arteries show clear evidence of laser-induced renal nerve damage without injury to the endothelium and part of the media. No evidence of selective nerve damage is observed using the 1210 nm and 1700 nm lasers with the current treatment parameters. Histochemical analysis of *in vivo* laser treatments in ovine renal arteries using a focused 980 nm laser show clear evidence of renal nerve damage with depths of damage extending > 1.5 mm from the artery wall. Sections with laser-induced damage to the media/adventitia at depths of > 1 mm without injury to the endothelium are also observed.

Conclusions: We demonstrate the use of focused lasers as an attractive energy source for causing renal nerve damage without injury to the artery wall and thus, may have potential therapeutic applications for conditions such as resistant hypertension, where renal denervation has been shown to be a promising form of treatment. Lasers Surg. Med. 46:689–702, 2014.

Key words: laser renal denervation; laser therapy; resistant hypertension

INTRODUCTION

Hypertension is a major global health concern with an estimated one third of the adult population in the developed world suffering from this condition [1,2]. Despite the availability of numerous effective pharmacologic agents and efforts to diagnose hypertension, only half of the treated patients are controlled to established blood pressure targets [2–4]. Using the National Health and Nutrition Examination Survey data collected from 2003–2008, Persell estimated the prevalence of resistant hypertension to be 12.8% of all US adults being treated for hypertension [5]. Pimenta *et al*., estimate a prevalence of resistant hypertension among patients treated for hypertension to be 15–30% based on results from clinical trials and more recent observational findings [6]. Effective pharmacology treatments may be limited by various factors

Conflict of Interest Disclosures: All authors have completed and submitted the ICMJE Form for Disclosure of Potential Conflicts of Interest and none were reported.
Contract grant sponsor: University of Michigan Cardiovascular Center Inaugural Fund.
*Correspondence to: Vinay V. Alexander, PhD, University of Michigan Electrical and Computer Engineering Solid State Electronics Laboratory 1301 Beal Avenue Ann Arbor, MI 48109, USA. E-mail: vinalex@umich.edu
Accepted 29 July 2014
Published online 29 August 2014 in Wiley Online Library (wileyonlinelibrary.com).
DOI 10.1002/lsm.22290

such as patient adherence, physician inertia, inadequate doses, inappropriate combinations of anti-hypertensive drugs, non-compliance with dietary restrictions, side effects of medications and drug ineffectiveness [7–9]. Thus, the development of new approaches for the management of hypertension that could potentially overcome these issues is a priority, especially for patients with so-called resistant hypertension, i.e. patients unable to achieve target blood pressure values despite multiple drug therapies at the highest tolerated dose and are at a high risk of major cardiovascular events [10,11]. A variety of studies have been performed, which suggests that hyper activation of the sympathetic nervous system plays an important role in initiating and maintaining hypertension [7,12,13]. Studies of renal denervation in animals performed using surgical and chemical techniques, have also further helped to establish the roles of renal sympathetic nerves in hypertension [14,15].

Recently, clinical studies in human patients have been performed to assess the safety and efficacy of a percutaneous catheter based approach (Symplicity^{TM}, Medtronic, CA) [10,16]. In this procedure, a specially designed catheter is inserted into the femoral artery, advanced into one of the renal arteries and the radio frequency (RF) energy is applied to the endoluminal surface to deliver thermal injury to the renal sympathetic nerves. In a safety and proof of principle study and in a separate randomized trial, this approach was shown to reduce blood pressure successfully, without serious adverse events in patients with resistant hypertension [10,16]. Durability of treatment effect up to two years has also been reported in a cohort of 153 patients with resistant hypertension treated using the catheter based RF denervation technique [17]. Recent publications have also confirmed the efficacy of renal denervation for the treatment of resistant hypertension [18–20].

Although well received by clinicians, there are limitations of renal denervation using the RF technique. Procedural limitations include the catheter instability, triggering frequent treatment interruptions, and the overall duration of the procedure, which consists of a minimum of eight 2 minute ablations, the time required to reposition the device continuously and the associated patient discomfort or pain [21]. While further research is necessary to assess long-term safety and efficacy of RF denervation, an underlying mechanism to cause renal denervation using RF has been attributed to a localized temperature rise or hyperthermia [22]. Morphological assessment of porcine renal arteries after RF denervation show acute transmural tissue coagulation and loss of endothelium resulting in local thrombus formation [23]. Vascular smooth muscle cells express what is called tissue factor (TF), a protein on their surfaces. Endothelial cells cover the smooth muscle cells in the renal artery preventing exposure of TF to proteins in the blood that initiate the clotting cascade. When endothelial cells are killed and removed from the wall, TF becomes accessible to clotting factors often resulting in thrombus formations [24–26]. While long-term studies of RF renal denervation claim almost completely re-endothelialized lumen [23], a treatment modality for renal denervation minimizing the duration of treatments and the acute loss of endothelium would still be desirable.

The experience with thermal injury to the endothelium and other non-target tissues has generated an interest in the exploration of alternative ablative energy forms. Recently, ultrasound therapy has been investigated as an alternate suitable modality for denervation of renal nerves [21,22]. Clinical trials have also been performed investigating the use of ultrasound (Paradise^{TM}, ReCor Medical, NY) for renal denervation. A percutaneous catheter based approach is used and consists of a cylindrical transducer that emits ultrasound energy circumferentially, once in the renal artery. A water balloon in the catheter is used to center the transducer in the artery and to cool the arterial wall to minimize damage to the endothelium and non-target tissue. Preliminary clinical studies using this technique have been performed on a cohort of 11 patients and indicate ultrasound therapy to be a promising treatment for resistant hypertension. In this case, an average of 5.1 ultrasound emissions was delivered in each subject for a total treatment duration of about four minutes [21].

Laser treatments are an alternative energy form widely used for a variety of medical therapeutic and diagnostic applications [27]. The recent availability of fiber coupled laser devices with sufficient average powers have led to the development of minimally invasive catheter based medical treatments [27–30]. Fiber lasers are potentially advantageous for renal denervation over other ablation techniques for the following reasons. First, fiber coupled lasers are available in high average powers ($>$40 W) and can be easily focused or collimated. Depending on the treatment delivery method (focused or collimated), the treatment site can be better confined and the total treatment time is likely to be less than both RF and ultrasound techniques, helping to reduce patient discomfort and pain during the procedure. Second, treatments using a focused laser set up could help in creating a temperature gradient along the depth of the treatment site, making it possible to damage target structures like the renal nerves with minimal injury to non-target structures like the endothelium without the use of an external cooling mechanism. Also, compared to RF and ultrasound with high penetration depths ($>$1 cm), the laser penetration depths can be easily limited by using the right wavelength, such that the depth of damage extends only as deep as that required to reach the renal nerves and ensures that the abdominal, pelvic or lower extremity nerves are unaffected. Finally, selective tissue damage using specific laser wavelengths have also been investigated in literature [31,32], which could prove to be attractive for causing selective nerve damage for renal denervation.

In this work, we present experimental results, which show that lasers are an attractive energy source for renal denervation. In vitro renal denervation using a focused 980 nm laser is performed in porcine and ovine renal arteries, where the histochemical analysis show that by

optimizing the treatment conditions, it is possible to damage the renal nerves without causing injury to the endothelium and part of the media. Then, we investigate the use of lasers at the lipid absorption lines, 1210 nm and 1700 nm, to cause selective damage to the renal nerves by targeting the lipid rich myelin sheaths surrounding the nerves. Next, *in vivo* renal denervation using a focused 980 nm laser is performed in sheep using a specially designed laser catheter and the histochemistry results show clear evidence of renal nerve damage with depths of damage extending >1.5 mm from the artery wall following a five second laser treatment. Evidence of adventitial damage at depths of >1 mm from the artery wall without injury to the endothelium and part of the media are also observed in some sections. Finally, we discuss possible improvements in the catheter design to provide better control of the position and treatment parameters inside the renal artery. Selective damage issues and other potential advantages of using lasers for renal denervation are also discussed before ending with our conclusions.

MATERIALS AND METHODS

This section is organized as follows. We first discuss the choice of wavelengths at 980 nm, 1210 nm, and 1700 nm for renal denervation based on the tissue absorption spectra and penetration depth calculations. Then, we provide details for the *in vitro* renal denervation experiments using a focused laser beam at the three wavelengths. Next, we explain the 980 nm laser catheter prototype design used for the ovine *in vivo* renal denervation experiments followed by details of the animal interventional procedures and the histochemistry protocol used to visualize live versus killed tissue for all samples in this paper.

Wavelength Selection and Penetration Depth Calculations

The primary requirement for the choice of wavelength is that it should be able to penetrate at least up to the depth in tissue to cause damage to the renal nerves, majority (>75%) of which are within ~1.5 mm from the lumen wall in humans [13]. In addition, it might be possible to cause selective damage to the nerves using specific laser wavelengths that target the nerves or nerve components with little or no damage to the non-target tissues. For example, wavelengths with strong lipid absorption could potentially target the lipid rich myelin sheaths [33] that surround the nerves and cause nerve injury with minimal collateral tissue damage.

For penetration depth calculations, we use the Beer's law in anisotropic media, where the fluence $\phi(z)$ falls exponentially with depth as given by $\phi(z) = \phi_0 \exp(-\mu_{eff} z)$; μ_a is the magnitude of the absorption coefficient, μ_s' is the reduced scattering coefficient and $\mu_s' = \mu_s(1-g)$, where μ_s is the scattering coefficient and g is the anisotropy coefficient. The reduced attenuation coefficient (μ_{eff}) and penetration depth (δ) are then calculated using the following formulas [34,35]:

$$\mu_{eff} = \sqrt{3\mu_a(\mu_a + \mu_s(1-g))} \quad \text{if } \mu_a << \mu_s';\ \mu_a < \mu' \tag{1}$$

$$\mu_{eff} = \mu_a + \mu_s(1-g) \quad \text{if } \mu_a \geq \mu' \tag{2}$$

$$\delta = 1/\mu_{eff} \tag{3}$$

The penetration depth is defined as the distance at which the fluence is reduced to 1/e of the incident value and is equal to $1/\mu_{eff}$. Since the tissue is mostly water, we assume for our calculations that the tissue absorption characteristics are similar to water. Since, scattering properties in the near infrared wavelengths are well documented for the dermis (compared to arterial tissue), we have used scattering coefficients in the dermis to calculate and compare the estimated penetration depths at the three wavelengths used in this study. Figure 1 shows the absorption spectra for water [36] and fat [37] and the scattering coefficient in the human dermis (http://omlc.ogi.edu/news/jan98/skinoptics.html; 1998). As seen in Figure 1, wavelengths around ~1700 nm and ~1210 nm are attractive for targeting lipid rich structures such as the myelin sheaths surrounding the renal nerves and at the same time are near relative water absorption minima, allowing for good penetration depths. On the other hand, 980 nm is an attractive wavelength for even deeper penetration depths, since it has the lowest water absorption of the three wavelengths, and is easily available in fiber coupled modules with high average powers of >30 W.

Table 1 shows the calculated attenuation coefficients and the penetration depths in tissue at 980nm, 1210 nm and 1700 nm, respectively. The penetration depths in tissue are calculated using equations [1–3] to be ~2.7mm,

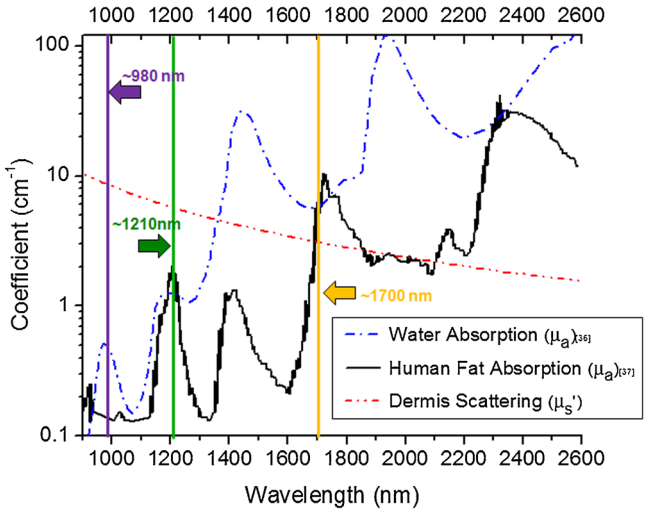

Fig. 1. Infrared spectra showing the coefficients for water (μ_a) and human fat absorption and effective scattering in the dermis (μ'_s).

TABLE 1. Estimated Penetration Depths in Tissue for 980 nm, 1210 nm and 1700 nm

Wavelength (nm)	μ_a (cm^{-1})	μ' (cm^{-1})	μ_{eff} (cm^{-1})	δ (mm)
980	0.5	8.5	3.7	~2.7
1210	1.3	5.8	5.3	~1.9
1700	6	3	9	~1.1

~1.9mm, and ~1.1mm for 980 nm, 1210 nm, and 1700 nm respectively. While all three wavelengths have penetration depths of >1 mm, only 980 nm and 1210 nm have the required penetration depth of > 1.5mm to damage majority of the renal nerves. Thus, the calculations presented here suggest that 980 nm and 1210 nm laser are more suitable for renal denervation than 1700 nm due to the deeper penetration depths. However, 1700 nm is potentially capable of causing more selective damage to the renal nerves than 1210 nm due to the higher lipid absorption and is included in our *in vitro* studies. Therefore, based on the penetration depths and potential for selective damage, the three wavelengths that we study for renal denervation in this paper are 980 nm, 1210 nm, and 1700 nm.

Table 2 shows a summary of the laser sources used in the renal studies. The 980 nm (IPG, USA), 1210 nm (QPC, USA), and 1700 nm (QPC, USA) lasers are all commercially available fiber coupled laser diodes. The 980 nm laser diode fiber has a core/cladding diameter of 105/125 microns, 0.22 fiber NA and a maximum output power of ~30W. The 1210 nm laser diode fiber has a core/cladding diameter of 400/440 microns, 0.22 fiber NA, and maximum output power of ~12W. The center wavelength is specified as 1211.76 nm with a spectral full width at half maximum (FWHM) of 4.59 nm at full power. The 1700 nm laser diode also has a core/cladding diameter of 400/440 microns, 0.22 fiber NA, and a maximum output power of ~7W. The center wavelength is specified as 1694 nm with a spectral width FWHM of 12 nm at full power.

Treatment Setup for *In-Vitro* Renal Denervation Experiments

The set up used for *in vitro* renal experiments is shown in Figure 2. An aspheric lens is used to focus the laser beam from the fiber output and the $1/e^2$ beam diameters along the beam are calculated using knife-edge measurements.

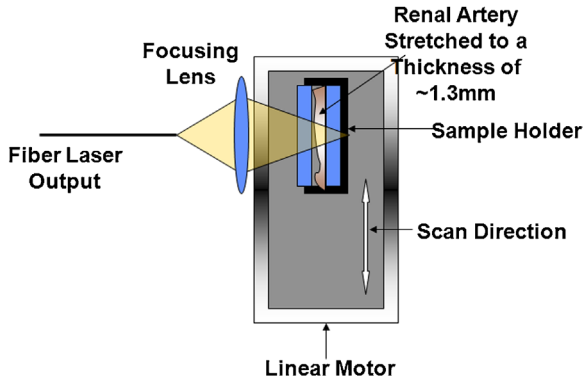

Fig. 2. Experimental setup used for the in vitro renal denervation studies using a focused laser beam.

The sample is mounted onto a sample holder attached to a computer controlled stepper motor stage with a minimum step size of 1 microns and scanned across the laser beam. Scanning is done in order to increase the area of laser treatment to maximize the chances of observing a laser affected nerve region after performing the sectioning and histochemistry analysis. For all *in vitro* experiments presented in this article, the scan speed is arbitrarily set to 0.4 mm/s and the incident power levels are optimized for the desired damage profile based on the histochemical analysis results.

In vitro renal denervation experiments are performed using both porcine and ovine renal arteries. Majority of the renal nerves (~75%) in humans are within ~1–1.5 mm from the artery wall. In our studies, we mimic this *in vivo* dimension, where the effects of blood pressure thin the lumen wall thickness and bring the nerves closer to the wall, by stretching the *in vitro* renal artery samples so that distance for the tissue top (lumen wall) to bottom (around the nerves) is ~1.3 mm. This is done by stretching the tissue sample between two glass slides with a ~1.3 mm spacer in between. Thus, for all the *in vitro* renal denervation, the thickness of the sections from the lumen wall to the bottom of the section is ~ 1.3 mm during the laser treatments. The *in vitro* denervation histochemistry results have a true/actual scale length included for comparison between sections, but is not an accurate representation of the depth during treatments.

The entire kidney and arteries along with a piece of aorta are obtained from a local butcher shop, kept in Dulbecco's

TABLE 2. Details of Laser Sources Used for the Renal Denervation Studies

Laser Source	Max Power (W)	Center Wavelength (nm)	FWHM at Full Power (nm)	Fiber Core/ Cladding Diameter (μm)	Fiber NA
980 nm	30	976	–	105/125	0.22
1210 nm	12	1211.76	4.59	400/440	0.22
1700 nm	7	1694	12	400/440	0.22

modified eagle medium (D-MEM), high glucose 1X (from GIBCO, CA), and transported to the laser lab within hours of extraction, where they are stored in a refrigerator at 5–7°C, until the experiments are performed. The samples are kept in a warm water bath at ~37°C for about an hour prior to the laser treatments. All treatments are performed less than 48 hours after obtaining the samples. For the *in vitro* experiments, the renal artery is cut into 3–4 sections and each section is then scanned across the laser with the beam incident on the lumen wall. Figure 3 shows an example, where the renal artery is extracted, sectioned and prepared for the in vitro laser treatments.Frozen sections of treated renal artery tissues are prepared and histochemical analysis is performed using the methylthiazolyldiphenyl-tetrazolium bromide (MTT) assay to identify laser damage in the sections [31].

Catheter Design for *In Vivo* Renal Denervation

The catheter distal end design used for the ovine *in vivo* studies is shown in Figure 4 and consists of five main components: a glass ferrule to hold the fiber output, an air gap to adjust focal length, a GRIN lens to focus the light, a right angle prism, and an outer steel tube enclosure. The final distal end is less than 1 cm in length and has an outer diameter (OD) less than 2.2 mm.

The first component is the glass ferrule, which is used to hold the optical fiber in place. The glass ferrule has an OD of ~1.8 mm and ID of ~0.129 mm to fit the 0.125 mm cladding fiber and is polished down using a diamond grinder to a length of ~2.2 mm to fit within our required length specifications. Figure 4 inset shows an example of a standard fiber-glass ferrule and a finished product. The fiber is held in place inside the ferrule using UV cured optical adhesive.

The next component is the air gap spacer between the fiber and the GRIN Lens (Edmund Optics, #64532, NJ). The focal distance between the outer steel tube and the focus is determined by adjusting the distance between the fiber end and the GRIN lens. The spacers are hypodermic steel tubes precision machined down to specific lengths. The spacer tubes have an OD of ~1.65 mm and an ID of ~1.58 mm. A GRIN lens is the focusing optic in this catheter design and has an OD of ~1.8 mm and a length of ~4 mm. Figure 5a shows the simulation results (using ZEMAX) for the range of focal lengths in tissue obtained using this GRIN lens for various air gap spacer lengths. Thus, a range of focal lengths can be obtained by adjusting the spacer lengths between the fiber and the GRIN lens. Figure 5b also shows the calculated beam diameters at the distal end output and at the focal spot. The distal end is assumed to be in contact with the artery wall and the refractive index in tissue is assumed to be 1.38 for the simulations.

The next component is the right angle prism (Tower Optical Corporation, FL) used to rotate the light by 90 degrees towards the renal artery wall. The prism is made of glass and the hypotenuse is aluminum coated to act like a mirror. The prism is glued on to the GRIN lens using UV cured optical adhesive.

The outer tube is the final component and holds all the optical components together. The hypodermic steel tube is

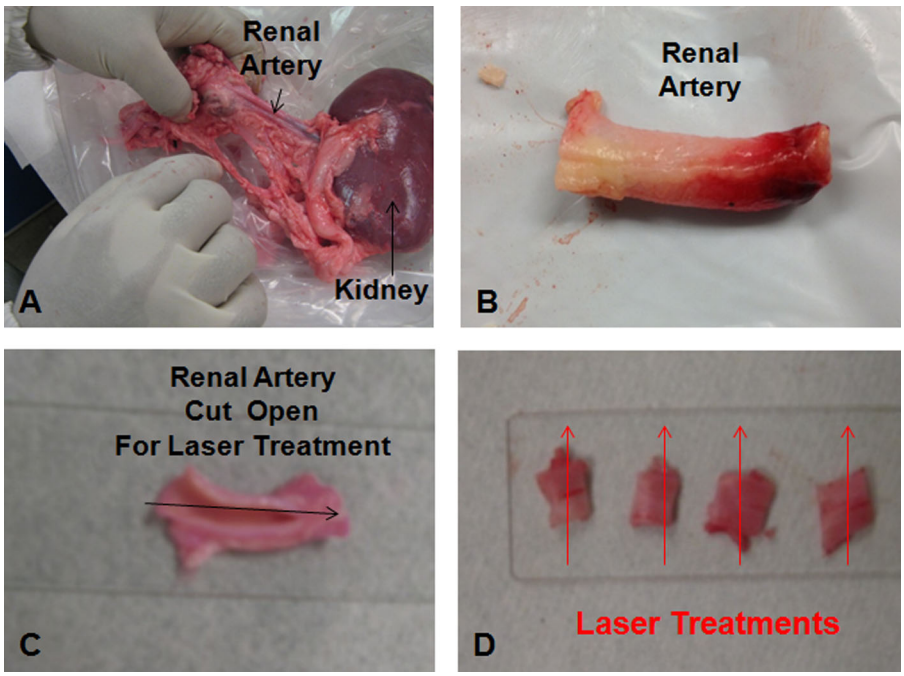

Fig. 3. Extraction of the renal artery and sample preparation for the *in vitro* experiments. The renal artery is first identified and extracted (**A**, **B**). The artery is then cut open, sectioned and prepared for laser treatments (**C**, **D**).

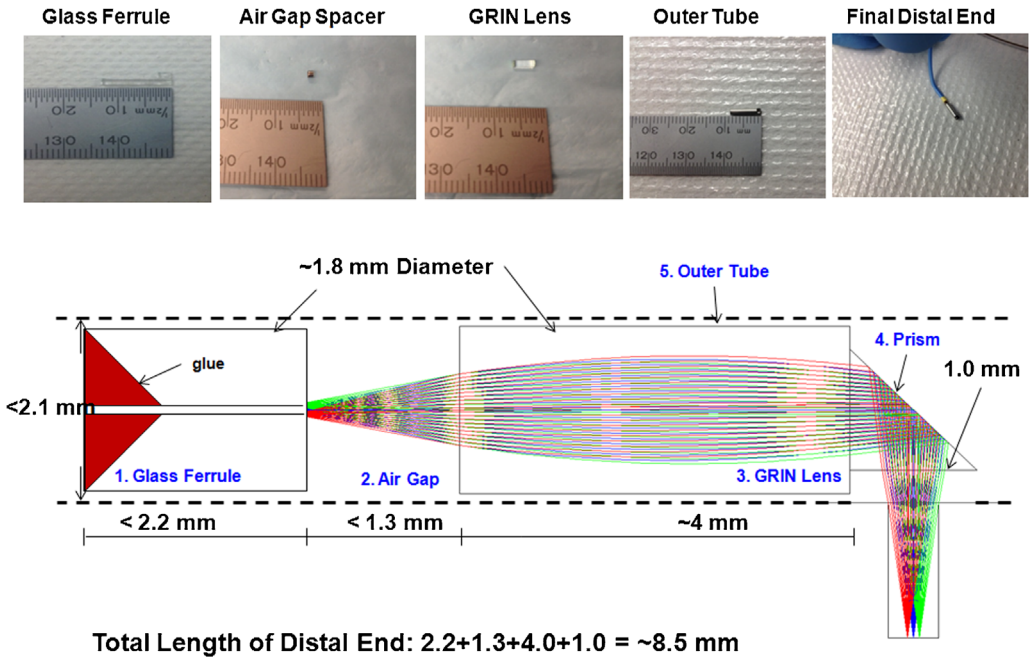

Fig. 4. Distal end design for the catheter used to deliver the *in vivo* treatments.

~8.5 mm long and has an ID of ~ 1.8 mm and an OD of less than 2.1 mm. The prism is protected by the outer tube and a 2 mm wide opening at the end of the tube allows the light from the prism to exit. The distal end and fiber is pushed though a braided polyimide tubing and glued to the metal outer tubing. The finished catheter is then guided through a 5 French (F) FR4 catheter to help provide stronger push ability in combination with the polyimide tubing. A Tygon tube model of the sheep aorta (1 cm diameter) and renal artery (0.5 mm diameter) are made to test and verify that the final catheter is able to fit within these dimensions. The fiber end is connectorized with an SMA connector to allow for a convenient connection with the laser source during treatments. The entire finished catheter is then packaged and sterilized using ethylene oxide prior to the *in vivo* experiments.

The current catheter prototype does not have any maneuvering ability once inside the renal artery. Thus,

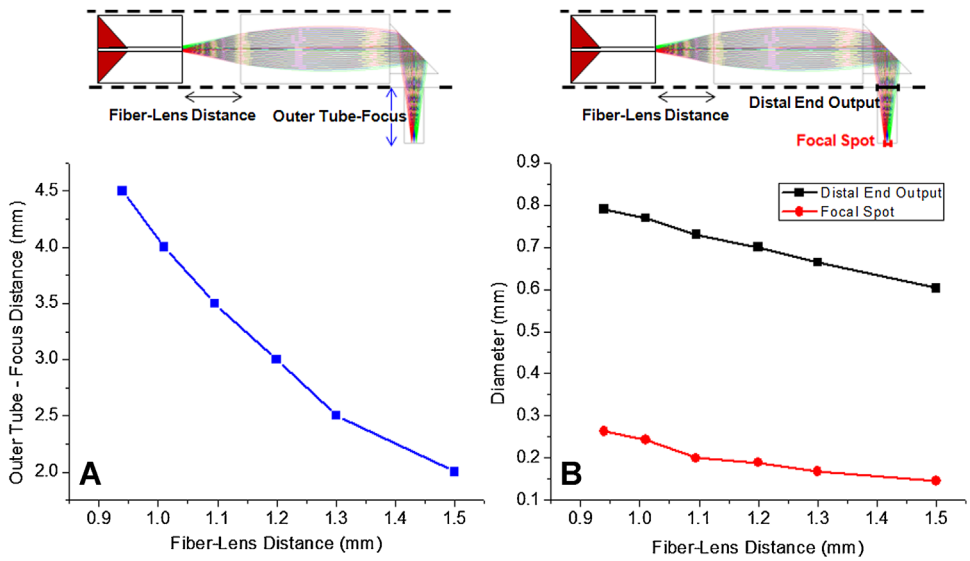

Fig. 5. ZEMAX Simulation results of the distal end performance in tissue (**A**) Outer tube–focus distance vs. the air gap length. (**B**) Estimate of the beam diameters at the distal end output and at the focus. The distal end is assumed to be in contact with the tissue.

we are not able to adjust the position such that the catheter is in the optimum position in the artery during the laser treatments. Since the treatments use a focused laser beam in order to damage the nerves with minimum impact on the endothelium, it is important for the focus to be close to the location of the renal nerves, majority of which lie in 1–1.5 mm region from the renal artery wall. One optimum condition for our treatment is for the distal end to make contact with the artery wall and then have the laser focus be at ~1.5 mm. Since, we are not able to control the distal end position once inside the artery; we use two catheter distal ends, each with a different focal length to improve our chances of getting close to the optimum condition. For the *in vivo* experiments, the two focal lengths in tissue (outer tube to focus) for the two catheters are estimated to be $\sim 2.8 \pm 0.3$ mm and $\sim 3.8 \pm 0.3$mm, respectively. The focal length measurements are performed in air and estimated using an aperture. The average diameter of the renal artery in sheep/goat is ~5mm (range from ~4 to 6 mm) and this choice of focal lengths might allow us to penetrate deep enough to achieve renal nerve damage and possibly save the endothelium as well. It is worth mentioning that we choose the two focal lengths to maximize our chances of getting close to the ideal condition of focusing close to the nerves, but the best way to guarantee this is to use a specifically designed catheter delivery system that is able to control and maneuver the position of the distal end within the renal artery cross section. Catheter design improvements are further explored in the discussion section.

Animal Interventional Procedures

The animal use protocol was reviewed and approved by the University Committee for the Use and Care of Animals. Three female adult sheep weighing 51–60 kg are used for the renal studies. The sheep are fasted for 24 hours prior to the procedure to aide in decreasing incidents of bloat, regurgitation, and to increase visualization during fluoroscopy. Each sheep is given pre-op Xylazine, 0.2 mg/kg intramuscular, to aide in calming the animal for restraint. An 18 g angiocatheter is placed in the cephalic vein, secured in place, and flushed with heparinized saline. Propofol, 4–6 mg/kg intravenous, is then administered for anesthetic induction and to aide in endotracheal intubation. A 10–11 mm endotracheal tube is used for intubation. The animals are then placed on oxygen and isoflurane anesthesia using an adult unilimb breathing tube and 3–4 L rebreathing bag. Ophthalmic ointment is placed in the eyes. The analgesics Buprenorphine 0.01 mg/kg intramuscular and Carprofen 4 mg/kg subcutaneous are given to aide in alleviating postoperative pain and swelling. The antibiotic Cefazolin 22 mg/kg intravenous is administered pre-operatively for prophylactic measures.

The animals are then transferred to the operating suite and placed on a fluoroscopy table in ventro-dorsal position. A Surgivet Advisor is utilized to monitor non-invasive blood pressure, EKG, pulse rate, oxygen saturation, respiratory rate, body temperature, and end tidal carbon dioxide. Reflexes are checked periodically. Lactated ringers are given intravenously at 10 ml/kg/hour throughout the procedure. A rumen tube is placed and maintained during the procedure to aide in the prevention of bloat and regurgitation of rumen contents.

Prior to the laser treatments, a 6 F sheath is inserted in the right femoral artery after application of Lidocaine. A perclose device is used to pre-close the artery [38]. An 8 F 45 cm arrow sheath is then introduced through the arteriotomy. Heparin in the dose of 100 IU/kg was administered. Through the arrow sheath, a 5 French FR4 or an IMA catheter is used to engage the renal artery. A Rosen wire is then advanced into the renal artery and the diagnostic catheter (FR4 or IMA) is advanced into the renal artery. Over the wire and the diagnostic catheter, the arrow sheath is advanced into the distal renal artery. The diagnostic catheter and the wire are removed and the laser catheter gently advanced out of the sheath and up to the renal artery bifurcation if possible. The treatment time is arbitrarily set for five seconds and the laser power delivered is varied over a range of power levels. All power levels reported are measured power at the fiber output. The catheter and sheath is slowly withdrawn back in steps of approximately 5 mm and treatments provided until the catheter is in the aorta. Attempts are made to turn the catheter as it is withdrawn with the intent of providing treatment along a spiral, but this could not be reliably done. All three animals survived the procedure and were allowed to recover for ~24 hours post laser treatment.

The sheep are sedated with 0.3 mg/kg intramuscular Xylazine and humanely euthanized ~24 hours after the laser procedure with intravenous sodium pentobarbital at a dose of 1 ml/4.5 kg body weight. The sheep are placed in left lateral recumbency and the body wall is opened. Surrounding viscera is removed, exposing the kidneys and abdominal aorta. The abdominal aorta and vena cava are incised cranial and caudal to the branch points of the renal arteries and veins, allowing removal of the kidneys and their major vascular attachments en bloc. The renal arteries are finely dissected from the attachments at the abdominal aorta and the renal hilus. A thin layer of adventitial adipose tissue is retained with the renal arteries to avoid inadvertent damage of small adventitial blood vessels (vasa vasorum).

The harvested renal arteries are placed in optimal cutting temperature compound (OCT^{TM}), frozen in liquid nitrogen and stored at -80°C until frozen sections can be cut. Total time from euthanasia to renal artery placement in media is approximately 20–30 minutes. Cryostat-cut sections are made and mounted on glass slides, and stored at -80°C until used for histochemical staining of dehydrogenase activity. To identify laser damage in the processed sections, we use the MTT histochemical assay, a proxy for dehydrogenase enzyme activity for cell viability [31]. Cells that are alive when frozen maintain dehydrogenase activity, but cells that are dead do not have this activity. In live cells that are frozen, dehydrogenase activity reduces the slightly yellow water soluble MTT substrate

into a water insoluble dark blue to black precipitate. Thus, in the MTT histochemical assay, live cells stain dark blue while dead cells remain clear. The volume of incubation medium is adjusted proportionally depending on the number of sections to be stained. The sections are immersed in MTT incubation medium under aerobic conditions with no ambient light for about 30 minutes, rinsed in DI water and dried afterwards. The sections are examined using a microscope (WILD Makroscop M420) and photos are taken using a digital camera (NIKON Coolpix 5000).

EXPERIMENTAL RESULTS

In vitro results at 980 nm, 1210 nm, and 1700 nm are presented first, followed by *in vivo* results at 980 nm using the designed laser catheter prototype.

In Vitro Laser Renal Denervation using a Focused 980 nm Laser

In-vitro renal denervation studies using the focused laser set up at 980 nm are performed in both porcine and ovine renal arteries. The renal arteries are exposed to a range of incident power levels, causing anywhere from little or no damage to complete damage of the entire artery section. In each case, the artery tissue is stretched during laser treatments so that the top to bottom thickness is ~1.3 mm, and the beam diameters on the tissue top (artery wall) and tissue bottom (adventitia) are estimated to be ~1.2 mm and ~0.4 mm respectively.

The MTT histochemistry results for porcine renal artery cross sections treated over a range of incident power levels at 980 nm are shown in Figure 6. Figure 6A shows an example where the treatment parameters (1.5 W, 0.4 mm/s scan) are inadequate to cause any damage to the renal artery tissue. Figure 6B shows an example of the optimum treatment condition (1.8W, 0.4 mm/s scan), where we are able to observe renal nerve damage with no injury to the endothelium and finally, Figure 6C shows a treated artery section where the power level (3W, 0.4 mm/s scan) is high enough to cause transmural damage to the entire renal artery tissue section from top to bottom at the treatment site. Thus, the results presented in Figure 6 show that by optimizing the laser treatment parameters, a focused laser beam at 980 nm can achieve renal nerve damage with little to no injury to the endothelium and part of the media.

Adult sheep are used as the animal model for our *in vivo* trials, since the aorta and artery diameters in sheep are closer in dimension to humans. Renal studies have also been reported in literature using the sheep as the animal model [39]. Therefore, in addition to the *in vitro* treatments in porcine renal arteries shown in Figure 10, we also performed *in vitro* renal denervation experiments in ovine renal arteries using the 980 nm [not presented in this article]. The MTT histochemistry results in sheep are seen to be consistent with *in vitro* porcine renal denervation results from Figure 10 and clearly show that a focused laser beam at 980 nm can be used to damage the renal nerves with little to no injury to the endothelium and part of the media. As an added advantage, 980 nm lasers are also commercially available in fiber coupled diode modules with average powers of > 30 W.

In Vitro Laser Renal Denervation Using Focused 1210 nm and 1700 nm Lasers

Laser sources near 1210 nm and 1700 nm are of interest for medical applications due to the higher absorption coefficient of lipids compared to that of water at these wavelengths, which suggests that it might be possible to selectively target lipid rich tissues with minimal damage to the surrounding non-target tissues using these wavelengths [31,32,37]. Since the myelin sheaths surrounding the nerves are rich in lipid content, it might be possible to selectively cause renal nerve damage with minimal damage to the surrounding tissues using lasers with wavelengths around 1210 nm and 1700 nm.

In-vitro renal denervation studies at 1210 nm and 1700 nm are performed in porcine renal arteries using the focused laser set up, where the renal arteries are exposed to a range of incident power levels, causing anywhere from little or no damage to complete damage of the entire section. In each case, similar to the previous section, the artery tissue is stretched during laser treatments so that the top to bottom thickness is ~1.3mm, and the beam diameters on the artery wall (tissue top) and

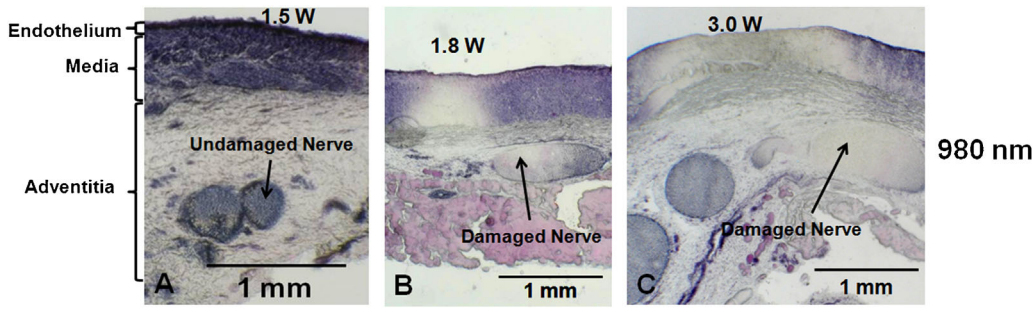

Fig. 6. In vitro porcine renal denervation results using the focused laser setup at 980 nm showing (**A**) insufficient damage (1.5 W, 0.4 mm/s scan), (**B**) Optimum condition with renal nerve damage without injury to the endothelium and part of the media (1.8 W, 0.4 mm/s scan) and (**C**) Excess damage with injury along the entire tissue depth (3 W, 0.4 mm/s scan).

adventitia (tissue bottom) are estimated to be ~1.2 mm and ~0.4 mm, respectively.

Figure 7 shows the MTT histochemistry results for porcine renal artery cross sections treated with the both wavelengths over a range of incident power levels. For each wavelength, the first column shows an example where the treatment power is inadequate to reach the nerves, the middle column shows an example of the optimum condition, where we are able to observe nerve damage with little to no injury to the endothelium, and finally, the last column shows an example, where the power level is high enough to cause transmural damage to the entire section from top to bottom at the treatment site. For example, Figure 7(A, B, C) shows the histochemistry results for treatments with the 1210 nm laser. Slight tissue damage is observed in Figure 7A (1.5W, 0.4 mm/s scan). In Figure 7B (1.8W, 0.4 mm/s scan), we see clear evidence of nerve damage with little to no damage to the endothelium. Fig 7C (2.1W, 0.4 mm/s scan) shows a section, where the higher incident power causes transmural damage at the treatment site. Similarly, Figure 7(D, E, F) shows the histochemistry results for artery sections treated with the 1700 nm laser.

The results in Figure 7, show that both 1210 nm and 1700 nm lasers are capable of causing renal nerve damage, with little to no injury to the endothelium and part of the media. However, the 1700 nm laser is only capable of causing partial nerve damage due to the higher absorption and lower penetration depth in tissue at this wavelength. The results shown in Figure 7 also do not show any clear evidence of selective nerve damage using current laser treatment parameters at 1210 nm and 1700 nm. Selectivity issues are further explored in the discussion section.

For the focused denervation experiments, Beer's law and the focus advantage are countering effects, i.e. if the absorption is high, then most of the light will be absorbed close to the lumen and not be able to penetrate deep enough to reach the nerves making the focusing advantage less useful. This can be further understood using a simple 1D Gaussian beam model taking into account both the effects of focusing, absorption, and scattering. The laser intensity distribution with tissue depth can be estimated by:

$$I(r,z) = I_{peak} e^{(-2r^2/w^2(z))} e^{(-\mu_{eff} z)}$$

where

$$I_{peak}(z) = 2\frac{P_{inc}}{\pi w^2(z)}$$

P_{inc} is the incident power on the tissue surface, $w(z)$ is the beam waist radius. For a converging laser beam of radius R0 at the tissue surface, focused at a depth $z = FD$ with a beam radius of RD at the focal spot, the beam waist

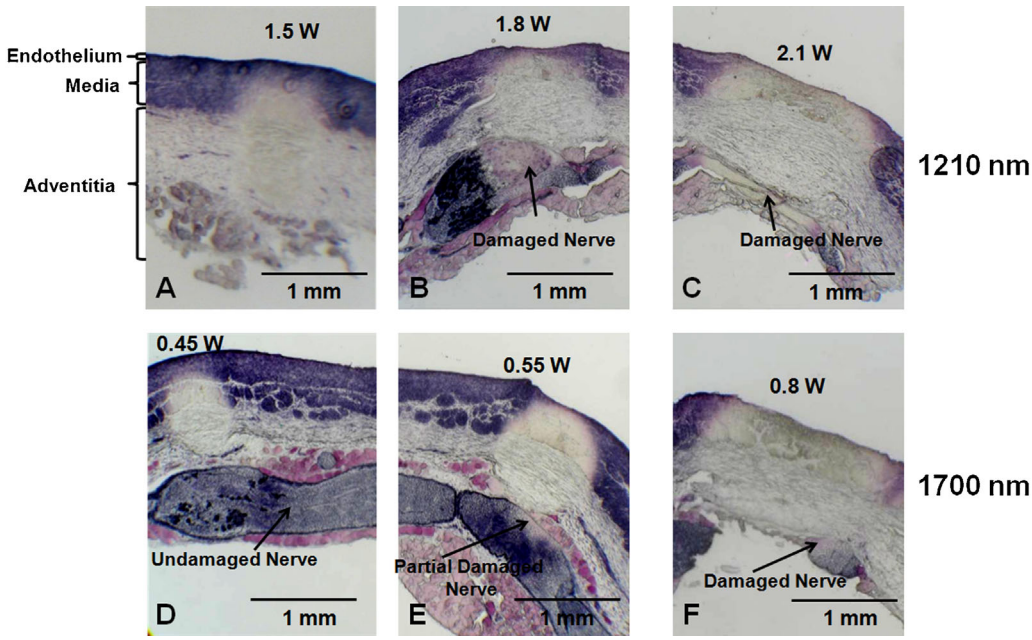

Fig. 7. In vitro porcine renal denervation results using the focused laser setup at 1210 nm (**A**, **B**, **C**) and 1700 nm (**D**, **E**, **F**), scanned at 0.4mm/s. Three cases are shown for each wavelength The first column shows inadequate damage. The middle column shows the optimum treatment condition achieved for each wavelength with laser damage to the nerves and no injury to the endothelium. The third column shows treatment power levels high enough to cause transmural damage extending across the entire section depth.

(w(z)) with depth can be estimated by the following expression:

$$w(z) = R0\left(\begin{array}{ll}\dfrac{(RD-R0)z}{R0\times FD}+1 & if\ 0\le z\le FD\\ \dfrac{(R0-RD)z}{R0\times FD}-\dfrac{(R0-2RD)}{R0} & if\quad z>FD\end{array}\right)$$

For the *in vitro* experiments shown in Figures 6 and 7, The values for R0 and RD are ~0.6mm and ~0.2 mm, respectively. In the absence of absorption and scattering, one would then expect a peak intensity difference along the beam center ($r=0$) of ~9× between the endothelium and the renal nerves. Once the effects of absorption and scattering (from section "Wavelength Selection and Penetration Depth Calculations") are taken into account, the intensity difference factor drops to ~6× for 980 nm, ~4× for 1210 nm, and ~3× for 1700 nm. Therefore, Beer's law and focusing advantage are seen to be countering effects and a lower effective attenuation is expected to be better for focusing applications at greater depths. Since 980 nm has the lowest effective attenuation, among three wavelengths considered, we can then expect to achieve the greatest intensity difference between the endothelium and the nerves at this wavelength.

In Vivo Renal Denervation Using a 980 nm Laser

A catheter-based approach (described in section "Catheter Design for *in vivo* Renal Denervation") is used to deliver the 980 nm laser treatments to the renal arteries in sheep. Two catheters with focal lengths of $\sim 2.8 \pm 0.3$ mm (FL1) and $\sim 3.8 \pm 0.3$ mm (FL2) in tissue are used for the *in vivo* renal denervation experiments. The laser output powers range from 2.0 to 4.0 W with a treatment time of five seconds at each treatment spot. The treatments are first administered in the renal artery section proximal to the kidney and then moved progressively to the distal end closer to the aorta. Figure 8 shows the fluoroscope images of the laser catheters in the renal artery prior to the laser treatments.

Figure 9 shows the MTT histochemistry for sections of ovine renal artery treated with the 980 nm laser (five seconds exposure time) using FL1 at 3.5–4.0 W (A, B), and FL2 at 2.5–3W (C, D). In Figure 9 (A and B), we see a distinct large nerve around the renal artery that is clearly damaged, as evidenced by the lack of staining. The depth of damage in this section is seen to extend > 1.1 mm from the artery wall. Figure 9(C and D) show another example, where the renal nerves in the treatment site are not stained and indicate thermal damage by the 980 nm laser. The depth of damage in this section is seen to extend >1.5 mm from the artery wall. The *in vivo* results presented in Figure 9 clearly indicate that the 980nm penetrates deep enough (>1.5 mm) to cause thermal damage to the renal nerves and that it is possible to achieve renal denervation using this technique. Figure 9 also shows some sections with a circumferential damage pattern, which could be the result of inadvertent catheter movements inside the renal artery.

While both examples in Figure 9 show evidence of laser renal denervation using the 980 nm laser, the endothelium is unstained as well indicating thermal injury. The laser treatments are delivered in a focused beam with a Gaussian profile, where the intensity is highest at the beam center and increases towards the focus. The results presented in Figure 9 show the endothelium to be damaged as well indicating that the beam intensity delivered to the artery wall must be higher than the damage threshold for the endothelium and media. Since the position of the distal end inside the renal artery cannot be controlled for our current catheter prototype, one potential reason for damage to the endothelium and media is that the focal point is closer to the artery wall instead of the nerves and there is a lack of sufficient laser intensity difference between the artery wall and nerve site.

Focusing the laser beam at a depth close to the renal nerves should allow for an intensity difference and hence, a

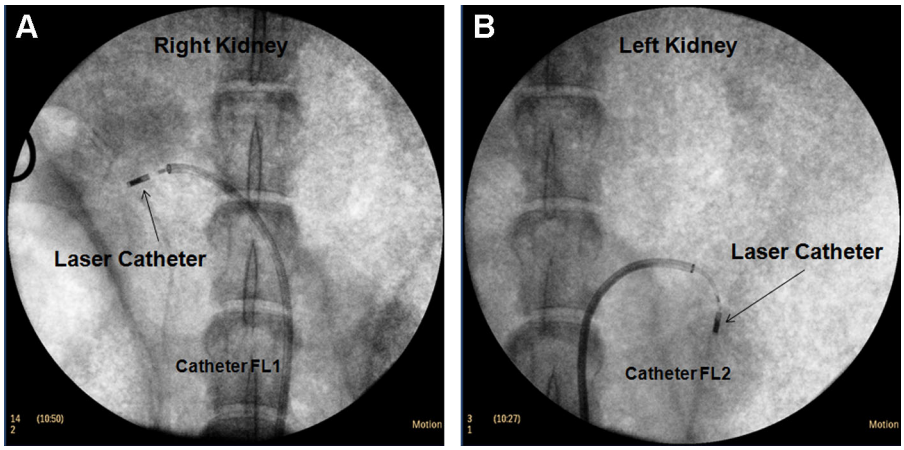

Fig. 8. Fluoroscope images of laser catheters in sheep in vivo (**A**) Catheter FL1, right kidney (**B**) Catheter FL2, Left kidney.

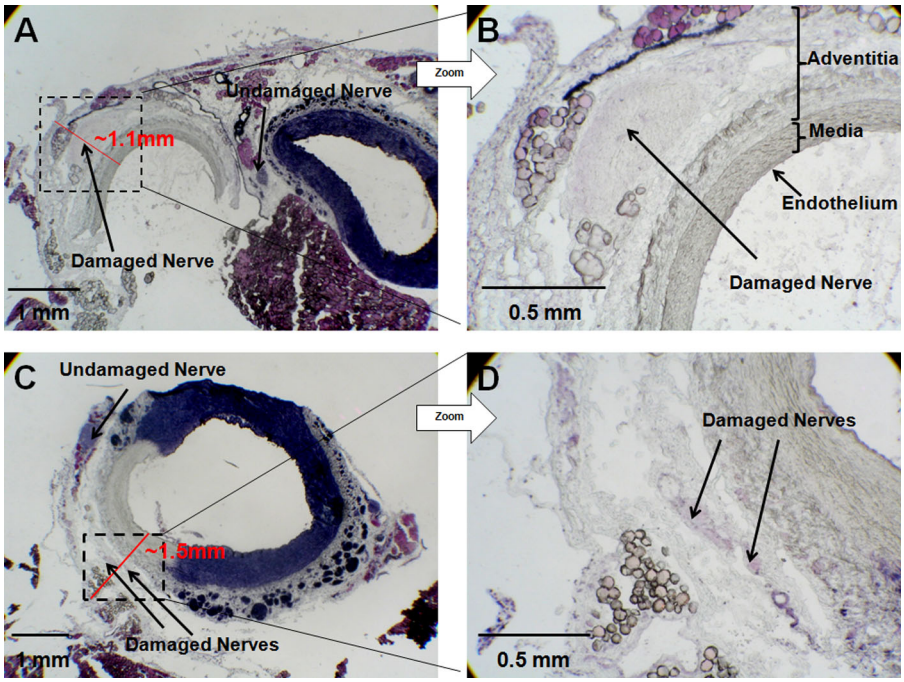

Fig. 9. MTT histochemistry of sections from *in vivo* trials showing complete renal denervation with 980 nm laser after treatment with (**A**, **B**) catheter FL1 3.5-4W, 5 second exposure and (**C**, **D**) catheter FL2, 2.5-3W, 5 second exposure.

temperature difference between the tissue top, close to the endothelium, and the tissue bottom, where the nerves are located. Thus, a focused laser beam treatment should be able to cause thermal damage to the renal nerves, while sparing injury to the endothelium and part of the media. Figure 10 shows examples of some sections from our *in vivo* experiments, where we see histological evidence of thermal damage in the media and adventitia without any damage to the endothelium. However, in these cases, there are no clearly identifiable renal nerves or the depth of damage does not extend deep enough to damage the renal nerves. Some possible reasons for the depth of damage not extending deep enough could be that the laser treatment power/exposure time may not have been sufficient and/or the focal spot may not be near the nerves, but closer to the media. While we have not observed in vivo histochemistry results showing clear nerve damage without injuring the endothelium, the results presented in this section show that it is possible to achieve renal denervation *in vivo* (Fig. 9) and the results presented in Figure 10 suggest that the focused laser treatment can cause arterial damage at depths $> \sim 1$ mm without causing damage to the renal artery wall including the endothelium and part of the media.

DISCUSSION AND CONCLUSIONS

Renal denervation has recently become of great interest as a potential treatment for resistant hypertension. The current treatment modalities use either RF or ultrasound therapy. Both of these techniques either cause endothelial

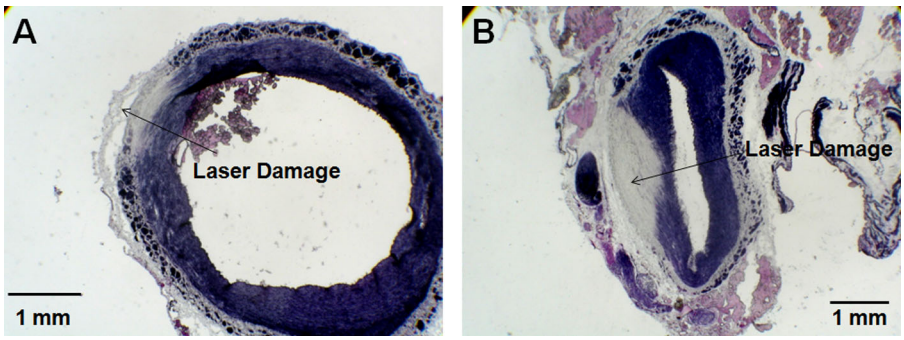

Fig. 10. In vivo MTT histochemistry examples showing laser damage to the media/adventitia with no injury to the endothelium and artery wall after 980 nm laser treatment with (**A**) catheter FL1 3.5-4 W, 5 second exposure and (**B**) catheter FL1, 2-2.5 W, 5 second exposure.

damage and local thrombus formation, or employ an external cooling mechanism to minimize the artery wall damage. In addition, their current energy delivery times are greater than four minutes [10,21]. There is an interest in exploring other energy forms for renal denervation that could substantially reduce the treatment times as well as minimize the damage to the endothelium and other non-target arterial tissue. Lasers have been widely used for medical ablation applications and have the following potential advantages. First, the treatment times can be significantly lower for laser treatments. The *in vivo* histochemistry results using the 980 nm laser presented in section "In vitro Laser Renal Denervation using a Focused 980 nm Laser" show that it is possible to damage renal nerves using lasers and the treatment time at each spot is only five seconds. With an estimated total of 4–6 treatment spots in each artery, the total energy delivery time could be less than one minute for the denervation treatments, helping to minimize patient discomfort and pain. Second, as seen in the in vitro results using focused laser beams in sections "In vitro Laser Renal Denervation using a Focused 980 nm Laser" and "In vitro Laser Renal Denervation using Focused 1210 nm and 1700 nm Lasers", lasers can be easily focused to create an intensity gradient across the artery section and allow saving the endothelium and part of the media without using any external cooling mechanism. Also, compared to RF and ultrasound with high penetration depths (>1 cm), the laser penetration depths as calculated in section "Wavelength Selection and Penetration Depth Calculations" show that by using the right wavelength, the depth of damage can be limited to be only as deep as that required to reach the renal nerves and ensures that the abdominal, pelvic or lower extremity nerves are unaffected.

Another advantage of using lasers is the potential for causing selective tissue damage by choosing the appropriate wavelengths. Since the myelin sheaths surrounding the nerves are rich in lipid content, it might be possible to selectively target the myelin sheaths to damage the renal nerves. As shown in Figure 1, both ~1700 nm and ~1210 nm are close to strong lipid absorption lines. However, the ratio of the absorption coefficient for water and lipids is still small at these wavelengths. Our preliminary *in vitro* work in renal arteries comparing these wavelengths as shown in section "In vitro Laser Renal Denervation using Focused 1210 nm and 1700 nm Lasers", show that ~1700 nm may not have the necessary damage depth to reach the renal nerves at ~1.5 mm without causing endothelial damage as well. We also did not observe any significant selective advantage of using the 1210 nm and 1700 nm over the 980 nm laser treatments. It is worth mentioning that the lipid absorption peak (from Fig. 1) is closer to 1720 nm and better selectivity might be achievable closer to this wavelength. However, the penetration depth will decrease further as we move closer to 1720 nm due to the higher water absorption. Increased selectivity at 1210 nm and at 1700 nm might be achievable by using altered pulse durations. For example, Sakamoto *et al* has reported selective damage to sebaceous glands in human skin with external cooling using a pulsed 1720 nm laser [32]. The optimal pulse duration for selective damage should be made shorter than or equal to the thermal damage time (defined as the time required for irreversible damage with sparing of the surrounding tissue) and is dependent on the target tissue structure and size (d). The thermal damage time is a function of the thermal relaxation time, $\tau \cong d^2/27\kappa$[40], where $\kappa$is the thermal diffusivity constant [40] and can be many times as long as the relaxation time of the target [41]. The nerve size and distribution varies significantly, from $<\sim 100\,\mu$m to $>\sim 1$ mm [22] and assuming aκ of 1.3×10^{-3}cm^2/s similar to [40], this corresponds to a thermal relaxation times ranging from ~3 ms to 300 ms across the cross section of the renal artery. Thus, the significant variations in nerve dimensions across the cross section of renal arteries might make selective denervation more challenging.

The *in vitro* experiments for renal denervation in sections "In vitro Laser Renal Denervation using a Focused 980 nm Laser" and "In vitro Laser Renal Denervation using Focused 1210 nm and 1700 nm Lasers" also suggest that wavelengths with lower tissue absorption might be more beneficial to leverage the focusing advantage and achieve denervation without damaging the endothelium. From this perspective, other wavelengths with lower tissue absorption, such as 1064 nm lasers could possibly be an even better candidate for renal denervation. However, the lower tissue absorption would also require a higher energy delivery to cause sufficient thermal alteration of the renal nerves and include the risk of causing damage beyond the intended tissue depths.

The *in vivo* results presented in section "In vivo Renal Denervation using a 980nm Laser" clearly show histological evidence of renal nerve damage after treatment with the 980 nm laser. However, the endothelium and artery wall is also injured in the current process. One of the major limitations in our animal trials is the catheter capabilities. The catheter prototype used in the *in vivo* trials currently does not have any maneuvering ability, once inside the renal artery. Thus, it is not possible for us to reliably know the position of the distal end within the artery and maneuver it such that it is at a known distance from the vessel wall. In our treatments, the same catheter depending on its location within the cross section of the vessel, could be focusing the light at the adventitia at one treatment spot and in the lumen at the other. In addition, a slight position change could result from a change in catheter position, respiratory movements of the kidney or even the pulsality of blood flow. The catheter movement could also result in inadequate exposure times and/or the overlap of treatment sites leading to insufficient damage or excessive damage at the treatment site. For example, the histochemistry results in Figure 9 seem to suggest a possible treatment spot overlap or distal end movement during treatment as evidenced by an almost circumferential damage profile. In addition, the actual power levels delivered to the artery wall could also depend on the amount of blood between the distal end and the artery wall.

Catheter maneuverability inside the renal artery plays a crucial role for renal denervation treatments including current treatments that use RF and ultrasound therapy. In these treatment modalities, the position of the catheter distal end is critical to obtain the desired results, since the power, exposure times and the required penetration are dependent on the distance between the energy source and the artery wall. One possible solution to fix the position of our laser catheter inside the renal artery is to use a technique similar to the RF treatments (http://www.medtronicrdn.com/intl/healthcare-professionals/symplicity-rdn-system/index.htm), where the laser distal end would be kept in contact with the renal artery wall prior to the laser treatments. The distal end contact with the artery wall can be monitored using the impedance measurements currently used in RF treatments. It might also be possible to ensure wall contact by monitoring the back reflection of laser light from the catheter. As the distal end gets closer to the artery wall, the light reflected back into the distal end from the artery wall will increase as well, which could be used to identify the position of the distal end within the artery. Another potential solution is to have the distal end enclosed in water or saline cooled balloon in contact with the artery wall, which would then enable the laser to be at a fixed distance from the artery wall while cooling the artery wall during treatments. As an example, laser treatments utilizing external cooling mechanisms have been successfully demonstrated in human skin to damage sebaceous glands at depths of $\sim$1.65 mm from the epithelium, while saving the top $>$0.5mm of the skin tissue from laser damage [31]. Therefore, the combined effect of cooling and focusing has a high potential to minimize endothelial and non-target tissue damage during the laser renal denervation treatments.

Since the exact position and distribution of the nerves within the renal artery during treatments are unknown, current denervation techniques use an algorithm to deliver treatments in a circumferential manner to ensure that the nerves are damaged. The laser treatments could be delivered circumferentially using a rotating mirror or mirror designs, where the incident light is split into a circumferential beam [42], which can then be used to damage the renal nerves and reduce treatment times further. In addition, it might be possible to image and detect the position of the nerves prior to the treatments. Catheter based OCT techniques are currently in existence and have been developed for arterial imaging, with penetration depths of $\sim$2–3 mm [43]. It remains unclear whether it is preferable to tailor the ablation to the proximal renal artery, where there are fewer larger nerve trunks or to the distal vessel, where there are more and smaller nerves. With a proximal strategy, missing a large nerve could compromise the therapeutic efficacy. On the other hand, a distal strategy would require treatment of a larger number of nerve targets to achieve complete denervation [13]. In both cases, identifying the renal nerves using an imaging technique like OCT, before laser treatments could help to reduce the number to treatment spots and improve efficacy by damaging a larger percentage of nerves while possibly avoiding unnecessary damage to the artery, all of which could help to reduce patient discomfort and pain.

In summary, we demonstrate a novel technique for renal denervation using focused infrared fiber lasers. Histochemical results for *in vitro* studies show that a focused laser set up can be successfully used to cause renal nerve damage without injuring the endothelium and part of the media. Catheter based *in vivo* renal denervation treatments in sheep using a 980 nm laser are performed and show clear evidence of renal nerve damage with depths of damage extending $>$ 1.5 mm from the artery wall. Laser induced damage to the media/adventitia at depths of $>$1 mm without injury to the endothelium are also observed *in vivo*. The results presented in this article indicate that lasers may offer a more efficient way to achieve renal denervation by shortening treatment times and minimizing damage to non-target tissues like the endothelium. Further research and clinical studies using lasers are warranted to determine the optimal treatment parameters for renal denervation and to evaluate their efficacy as a potential treatment for resistant hypertension.

ACKNOWLEDGEMENTS

The authors would like to thank the Unit for Laboratory Animal Medicine with sheep euthanasia and necropsy, particularly Laura Preiditsch and Dr. Ingrid L. Bergin of the Pathology Cores for Animal Research. We are also grateful to David Carter, Jim Tice and Michael Folts at the physics instrument shop and Roy Wentz at the Glass shop at the University of Michigan for their help in precision machining parts of the catheter used in this study. We would also like to thank Judy Poore and Jeff Harrison and the Histology Core of the Microscopy & Image Analysis Laboratory core facility at the University of Michigan Medical School for their help and guidance in preparing cryostat sections of the tissues presented in this study. The authors also thank Roel Beltran of the Cardiovascular Center at the University of Michigan for help with acquiring the medical supplies used in the animal trials. This project was funded by the University of Michigan Cardiovascular Center Inaugural Fund.

REFERENCES

1. Lloyd-Jones D, Adams R, Carnethon M, Simone GD, Ferguson TB, Flegal K, Ford E, Furie K, Go A, Greenlund K, Haase N, Hailpern S, Ho M, Howard V, Kissela B, Kittner S, Lackland D, Lisabeth L, Marelli A, McDermott M, Meigs J, Mozaffarian D, Nichol G, O'Donnell C, Roger V, Rosamond W, Sacco R, Sorlie P, Stafford R, Steinberger J, Thom T, Wasserthiel-Smoller S, Wong N, Wylie-Rosett J, Hong Y. Heart disease and stroke statistics—2009 update: A report from the American heart association statistics committee and stroke statistics subcommittee. Circulation 2009;119:480–486.
2. Kearney P, Whelton M, Reynolds K, Muntner P, Whelton P, He J. Global burden of hypertension: Analysis of worldwide data. Lancet 2005;365:217–223.
3. (WHO) WHO. Global health risks: mortality and burden of disease attributable to selected major risks. 2009.

4. Roger V, Go A, Lloyd-Jones D, Adams R, Berry J, Brown T, Carnethon M, Dai S, Simone Gd, Ford E, Fox C, Fullerton H, Gillespie C, Greenlund K, Hailpern S, Heit J, Ho P, Howard V, Kissela B, Kittner S, Lackland D, Lichtman J, Lisabeth L, Makuc D, Marcus G, Marelli A, Matchar D, McDermott M, Meigs J, Moy C, Mozaffarian D, Mussolino M, Nichol G, Paynter N, Rosamond W, Sorlie P, Stafford R, Turan T, Turner M, Wong N, Wylie-Rosett J. Heart disease and stroke statistics—2011 update: A report from the American Heart Association. Circulation 2011;123(4):e18–e209.
5. Persell SD. Prevalence of resistant hypertension in the United States, 2003–2008. Hypertension 2011;57:1076–1080.
6. Pimenta E, Calhoun DA. Resistant hypertension: Incidence, prevalence and prognosis. Circulation 2012;125:1594–1596.
7. Thomas G, Shishehbor MH, Bravo EL, Nally JV. Renal denervation to treat resistant hypertension: Guarded optimism. Cleve Clin J Med 2012;79(7):501–510.
8. Erdine S. Compliance with the treatment of hypertension: The potential of combination therapy. J Clin Hypertens 2010; 12(1):40–46.
9. Fergus I. Antihypertensive pharmacotherapy: Adverse effects of medications promote nonadherence. J Cardiometab Syndr 2009;4(1):E1–E3.
10. Krum H, Schlaich M, Whitbourn R, Sobotka PA, Sadowski J, Bartus K, Kapelak B, Walton A, Sievert H, Thambar S, Abraham WT, Esler M. Catheter-based renal sympathetic denervation for resistant hypertension: A multicentre safety and proof-of-principle cohort study. Lancet 2009;373:1275–1281.
11. Calhoun DA, Jones D, Textor S, Goff DC, Murphy TP, Toto RD, White A, Cushman WC, White W, Sica D, Ferdinand K, Giles TD, Falkner B, Carey RM. Resistant hypertension: diagnosis, evaluation, and treatment: a scientifi c statement from the American Heart Association Professional Education Committee of the Council for High Blood Pressure Research. Circulation 2008;117:e510–526.
12. Schlaich MP, Krum H, Sobotka PA, Esler MD. Renal Denervation and Hypertension. Am J Hypertens 2011;24(6): 635–642.
13. Atherton DS, Deep NL, Mendelsohn FO. Micro-Anatomy of the Renal Sympathetic Nervous System: A Human Postmortem Histologic Study. Clin Anat 2012;25:628–633.
14. Campese V, Ye S, Zhong H, Yanamadala V, Ye Z, Chiu J. Reactive oxygen species stimulate central and peripheral sympathetic nervous system activity. Am J Physiol Heart Circ Physiol 2004;287:(H695–H703).
15. Katholi R. Renal nerves in the pathogenesis of hypertension in experimental animals and humans. Am J Physiol 1983;245: (F1–F14).
16. Esler MD, Krum H, Sobotka PA, Schlaich MP, Schmieder RE, Böhm M. Renal sympathetic denervation in patients with treatment-resistant hypertension (The Symplicity HTN-2 Trial): a randomised controlled trial. Lancet 2010;376:1903–1909.
17. Krum H. Catheter-based renal sympathetic denervation for resistant hypertension: durability of blood pressure reduction out to 24 months. Hypertension 2011;57:911–917.
18. Krum H, Schlaich M, Sobotka P, Esler M, Mahfoud F, Böhm M, Dunlap M, Rocha-Singh K, Katholi R. TCT-12 Long-term follow-up of catheter-based renal denervation for resistant hypertension confirms durable blood pressure reduction. J Am Coll Cardiol 2012; 60.
19. Worthley S, Tsioufis C, Worthley M, Sinhal A, Chew D, Meredith I, Malaiapan Y, Papademetriou V. TCT-213 Safety and efficacy of a novel multi-electrode renal denervation catheter in resistant hypertension: 3 month data from the EnligHTN I trial. J Am Coll Cardiol 2012; 60.
20. Schlaich MP, Bartus B, Hering D, Mahfoud F, Böhm M, Lambert EA, Krum H, Lambert GW, Esler MD. 311 Feasibility of catheter-based renal denervation and effects on sympathetic nerve activity and blood pressure in patients with end-stage renal disease. J Hypertension 2012;30:e91–e92.
21. Mabin T, Sapoval M, Cabane V, Stemmett J, Iyer M. First experience with endovascular ultrasound renal denervation for the treatment of resistant hypertension. Eurointervention 2012;8:57–61.
22. Sinelnikov Y, McClain S, Zou Y, Smith D, Warnking R. Renal denervation by intravascular ultrasound: Preliminary in vivo study. AIP Conf Proc 2012;1481:337–344.
23. Steigerwald K, Titova A, Malle C, Kennerknecht E, Jilek C, Hausleiter Jr, hrig JrMN, Laugwitz K-L, Joner M. Morphological assessment of renal arteries after radiofrequency catheter-based sympathetic denervation in a porcinemodel. J Hypertens 2012;30:2230–2239.
24. Butenas S, Orfeo T, Mann KG. Tissue factor in coagulation which? where? when? Arterioscler Thromb Vasc Biol 2009;29:1989–1996.
25. Hinsbergh VWMv. Endothelium—role in regulation of coagulation and inflammation. Semin Immunopathol 2011;34:93–106.
26. Breitenstein A, Tanner FC, Lüscher TF. Tissue Factor and Cardiovascular Disease: Quo Vadis? Circ J 2010;74:3–12.
27. Peng Q, Juzeniene A, Chen J, Svaasand LO, Trond Warloe, Giercksky K-E, Moan J. Lasers in medicine. Rep Prog Phys 2008;71:056701.
28. Reddy VY, Neuzil P, d'Avila A, Laragy M, Malchano ZJ, Kralovec S, Kim SJ, Ruskin JN. Balloon catheter ablation to treat paroxysmal atrial fibrillation: What is the level of pulmonary venous isolation? Heart Rhythm 5:353–360.
29. Liu P, Ren S, Yang Y, Liu J, Ye Z, Lin F. Intravenous catheter-guided laser ablation: a novel alternative for branch varicose veins. Int Surg 2011;96:331–336.
30. Gerstenfeld EP. Have lasers finally found their niche in interventional cardiology? Heart 2012;98(7):525–527.
31. Alexander VV, Ke K, Xu Z, Islam MN, Freeman MJ, Pitt B, Welsh MJ, Orringer JS. Photothermolysis of sebaceous glands in human skin ex vivo with a 1,708 nm raman fiber laser and contact cooling. Lasers Surg Med 2011;43:470–480.
32. Sakamoto FH, Doukas AG, Farinelli WA, Tannous Z, Shinn M, Benson S, Williams GP, Gubeli JF, Dylla HF, R. Rox Anderson M. Selective photothermolysis to target sebaceous glands:Theoretical estimation of parameters and preliminary results using a free electron laser. Las Surg Med 2012;44: 175–183.
33. Morell P, Quarles RH. Characteristic Composition of Myelin. In: Siegel G, Agranoff B, Albers R, editors. *Basic Neurochemistry: Molecular, Cellular and Medical Aspects*. 6 ed. Philadelphia: Lippincott-Raven; 1999.
34. Maitland DJ, JrJTW, Prystowsky JB. Optical properties of human gallbladder tissue and bile. App Opt 1993;32(4):586–591.
35. Jacques SJ. Laser-Tissue Interactions. In: Schwesinger WH, Hunter JG, editors. *The Surgical Clinics of North America. Volume 72, Lasers in General Surgery*. Philadelphia: W. B. Saunders Company. 1992. 531–558.
36. Palmer K, Williams D. Optical properties of water in the near infrared. J Opt Soc Am 1974;64(8):1107–1110.
37. Anderson R, Farinelli W, Laubach H, Manstein D, Yaroslavsky A, Gubeli J, Jordan K, Neil G, Shinn M, Chandler W, Williams G, Benson S, Douglas D, Dylla H. Selective photothermolysis of lipid-rich tissues: A free electron laser study. Lasers Surg Med 2006;38(10):913–919.
38. Bhatt DL, Raymond RE, Feldman T, Braden GA. Successful "pre-closure" of 7Fr and 8Fr femoral arteriotomies with a 6Fr suture-based device (the Multicenter Interventional Closer Registry. Am J Cardiol 2002;89:777–779.
39. Whitworth JA, Denton DA, Graham WF, Humphery TJ, Scoggins BA, Coghlan JP. The effect of renal denervation on acthjnduced hypertension in sheep. Clin Exp Pharmacol Physiol 1981;8:203–207.
40. Parrish JA, Anderson RR, Harrist T, Paul B, Murphy GF. Selective thermal effects with pulsed irradiation from lasers: From organ to organelle. J Invest Dermatol 1983;80:75s–80s.
41. Altshuler GB, Anderson RR, Manstein D, Zenzie HH, Smirnov MZ. Extended theory of selective photothermolysis. Lasers Surg Med 2001;29:416–132.
42. Islam MN, Cheetah Omni LLC. assignee. Laser-based method and system for selectively processing target tissue material in a patient and optical catheter assembly for use therein. 2011.
43. Yan W, Ward MR, Nelson G, Figtree GA, Bhindi R. Overcoming limited depth penetration of optical coherence tomography with wire bias free J Am Coll Cardiol Intv 2012;5: e1–e2.